[7]P. C. Martin, in *Statistical Mechanics of Equilibrium and Non-Equilibrium*, edited by J. Meixner (North-Holland, Amsterdam, 1965), p. 100.

[8]If one is interested in higher nonlocal terms, one has to iterate Eq. (2.12c').

[9]R. E. Peierls, *Quantum Theory of Solids* (Clarendon, Oxford, 1955).

[10]There are also no projections on S^+ and S^- and the off-diagonal diffusion constants vanish too.

[11]T. Holstein and H. Primakoff, Phys. Rev. 58, 1098 (1940).

[12]T. Oguchi, Phys. Rev. 117, 117 (1960).

[13]F. Keffer, in *Encyclopedia of Physics* (Springer, Berlin, 1966), XVIII/2, p. 1.

[14]K. H. Michel and F. Schwabl, Physik Kondensierten Materie 11, 144 (1970). A short report on part of the present work has been given in K. H. Michel and F. Schwabl, Solid State Commun. 7, 1781 (1969).

[15]E. W. Prohofsky and J. A. Krumhansl, Phys. Rev. 133, A1403 (1964).

[16]L. P. Kadanoff and J. Swift, Phys. Rev. 166, 89 (1968).

[17]H. Mori and K. Kawasaki, Progr. Theoret. Phys. (Kyoto) 27, 529 (1962); K. Kawasaki and H. Mori, *ibid.* 28, 690 (1962); K. Kawasaki, *ibid.* 38, 1052 (1967).

[18]V. G. Vaks, A. I. Larkin, and S. A. Pikin, Zh. Eksperim. i Teor. Fiz. 53, 1089 (1967) [Soviet Phys. JETP 26, 647 (1968)].

[19]This is not necessarily in contradiction with Mori and Kawasaki[17] who evaluated $\Lambda(\vec{q})$ in the spin-wave region, using the time dependence of the free operators.

[20]V. N. Kashcheev and V. N. Krivoglaz, Fiz. Tverd. Tela 3, 1541 (1961) [Soviet Phys. Solid State 3, 1117 (1961)]; A. B. Harris, Phys. Rev. 175, 674 (1968).

[21]B. I. Halperin and P. C. Hohenberg, Phys. Rev. Letters 19, 700 (1967); Phys. Rev. 177, 952 (1969).

[22]R. A. Ferrell, N. Menyhard, H. Schmidt, F. Schwabl, and P. Szepfalusy, Phys. Rev. Letters 18, 891 (1967); Ann. Phys. (N. Y.) 47, 565 (1968).

[23]B. I. Halperin and P. C. Hohenberg (report of work prior to publication).

[24]A. I. Akhiezer, J. Phys. (SSR) 10, 217 (1946); A. I. Akhiezer, V. G. Bar'yakhtar, and S. V. Peletminskii, *Spin Waves* (North-Holland, Amsterdam, 1968).

[25]For an exhaustive review of relaxation processes in ferromagnets see Refs. 13 and 24.

[26]For temperatures where dipole forces are small but not negligible one could treat the magnetization similarly to the momentum as an approximately conserved quantity. This would give a second window condition.

[27]See, e.g., T. R. McGuire and M. W. Shafer, J. Appl. Phys. 35, 984 (1964).

[28]See, for instance, L. Van Hove, Phys. Rev. 95, 1374 (1954); P. G. de Gennes, *Magnetism*, edited by G. T. Rado and H. Suhl (Academic, New York, 1963), Vol. 3, p. 115.

[29]M. W. Shafer, T. R. McGuire, and J. C. Suits, Phys. Rev. Letters 11, 251 (1963).

[30]J. F. Dillon, Jr., and J. P. Remeika, J. Appl. Phys. 34, 637 (1963).

[31]H. L. Davis and A. Narath, Phys. Rev. 134, A433 (1964).

[32]We thank Professor S. Grossmann for a useful discussion on this point.

PHYSICAL REVIEW B VOLUME 2, NUMBER 1 1 JULY 1970

Raman Spectra and Mode Frequency Shifts of Ferroelectric Sodium Nitrite at 77 and 294°K

C. K. Asawa and M. K. Barnoski
Hughes Research Laboratories, Malibu, California 90265
(Received 9 February 1970)

The Raman spectra of the noncentrosymmetric biaxial sodium nitrite ($NaNO_2$) single crystal at 77 and 294 °K are presented. No major difference between the two spectra is observed, indicating that the recently reported phase transition at 178 °K from thermal-expansion measurements does not appear to change the crystal symmetry. Frequency shifts were observed with changes in the phonon wave-vector orientation for all five asymmetric B modes. The frequency shifts of the asymmetric internal vibrational $B_1(x)$ mode of the NO_2^- molecular ion were examined in some detail.

INTRODUCTION

Very little work has been done on the study of noncentrosymmetric biaxial crystals by Raman spectroscopy. The lack of theory, as well as the birefringence, makes the analysis of the data difficult at best. Ferroelectric sodium nitrite is one of the simplest orthorhombic biaxial crystals consisting of one molecule, four atoms, per primitive unit cell. The limited number of normal modes

makes it an ideal biaxial material from which to analyze Raman scattering.

Previous work[1-3] on Raman scattering appears to have been done with extended exciting sources so that complete definitive studies were not possible. In this experiment, the Raman scattering spectra of single-crystal $NaNO_2$ were measured using a highly directional and polarized laser source. Polarized spectra for various crystal orientations at 294 and 77°K are presented here. In addition, the Raman frequency shift of the internal asymmetric stretching vibration $B_1(x)$ of the nitrite molecular ion has been investigated as a function of the phonon wave-vector orientation in the crystal.

The space group for the ferroelectric phase of $NaNO_2$ is C_{2v}^{20}, while that for the paraelectric phase is D_{2h}^{25}. There is also an antiferroelectric phase[4] located in the narrow temperature range between the ferroelectric-to-antiferroelectric and antiferroelectric-to-paraelectric transition temperatures of 436.8 and 438 °K, respectively. Recent measurements[5] indicate that there is yet a third phase transition at 178 °K.

A standard analysis under a factor group representation of C_{2v}^{20} reveals that there are nine normal modes in the ferroelectric phase, all of which are Raman active. Of the eight infrared active modes, five are lattice vibrations of the sodium against the nitrite ion and three are the internal molecular normal modes of the planar nitrite ion. The temperature dependence above 300°K of all eight infrared-active modes has been recorded in the infrared.[6,7] The nomenclature of the irreducible representations of C_{2v}^{20} along with the coordinate system used here is the same as that of Ref. 6.

EXPERIMENTAL PROCEDURE

The standard laboratory arrangement, consisting of a 1-W cw argon laser, polarizer, double monochromator, and a photomultiplier pulse-counting system, was used. The 5145-Å laser line was principally employed.

Single-crystal $NaNO_2$ was grown by solidification from the melt and oriented by utilizing the well-known cleavage planes. The desired orientations were achieved by mounting samples in a jig which was designed to accept crystals which possessed angles corresponding to those between cleavage planes. The samples were then ground and polished with a smooth, rotating, bakelite disk slightly moistened with water. The orientational accuracy was within 1°. Because the crystals tend to cleave when suddenly immersed into liquid nitrogen, slow precooling was necessary for the 77° K runs.

EXPERIMENTAL RESULTS AND DISCUSSION

Complete Raman Spectra at 294 and 77°K

Complete Raman spectra measured at 294 and 77°K for various orientations and polarizations of the exciting and scattered radiation in terms of the crystallographic axes are shown in Figs. 1 and 2, respectively. Sufficient data have been obtained at both temperatures to display all six polarizability tensor components associated with a body-centered orthorhombic bravais lattice. The results are for right-angle scattering. Notations of the type $x(yx)z$ are now standard and are to be interpreted as follows: $x(yx)z$ means that the incident light is propagated in the x direction (first letter) while polarized in the y direction (second letter), and the scattered light is propagated in the z direction (fourth letter) while polarized in the x direction (third letter). For easy reference, the Raman polarizability tensors[8] for the point group C_{2v} are listed below:

$$A_1(z)\begin{pmatrix} a & 0 & 0 \\ 0 & b & 0 \\ 0 & 0 & c \end{pmatrix}, \quad A_2: \begin{pmatrix} 0 & d & 0 \\ d & 0 & 0 \\ 0 & 0 & 0 \end{pmatrix},$$

$$B_1(x)\begin{pmatrix} 0 & 0 & e \\ 0 & 0 & 0 \\ e & 0 & 0 \end{pmatrix}, \quad B_2(y): \begin{pmatrix} 0 & 0 & 0 \\ 0 & 0 & f \\ 0 & f & 0 \end{pmatrix}.$$

The frequencies of the fundamental normal modes are designated in each spectrum. For comparative purposes these results are compiled in Table I. As can be seen in the table, all the expected Raman lines are observed, with the exception of the $A_1(z)$ translational vibration. The mode assignments, types, and frequencies are in general agreement with the room-temperature results reported previously.[6] The extra lines that are not affixed with wave numbers in Figs. 1 and 2 result primarily from depolarizations of the fundamental lines resulting from scattering from slight crystal imperfections. All these extra lines are weak compared with the fundamental modes, with the possible exception of those which stem from the unusually strong A_2 mode [see, for example, the line at 121 cm^{-1} in the $z(xx)y$ and $z(yy)x$ spectra of Fig. 1 and the corresponding line at 127 cm^{-1} of

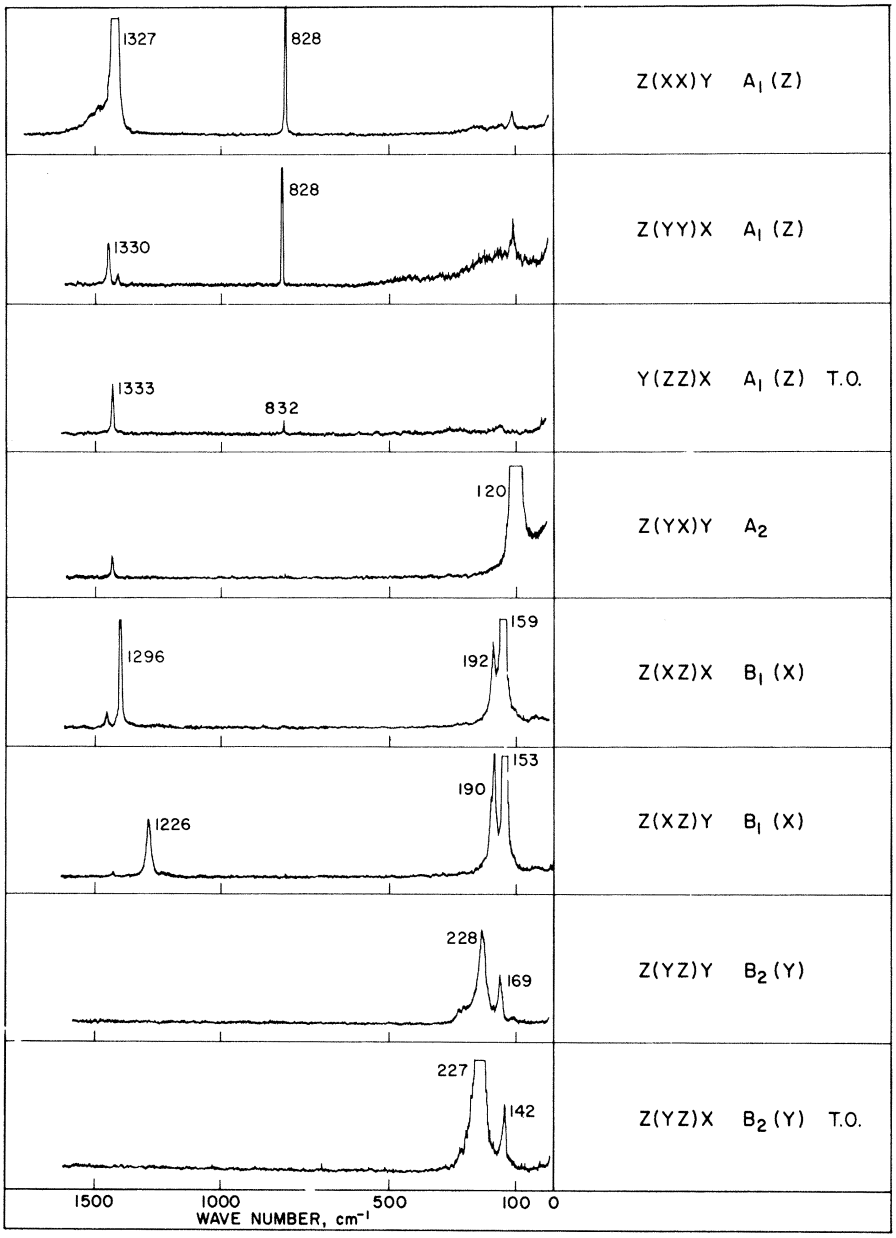

FIG. 1. Raman spectra of $NaNO_2$ at 294 °K for various orientations and polarizations of the incident and scattered light beams.

Fig. 2].

Inspection of the spectra associated with the polarizability tensor component α_{yy} [$z(yy)x$ spectra in Figs. 1 and 2] reveals that in the ferroelectric phase there is a broad band extending from approximately 40 to 200 cm^{-1}, which disappears as the temperature is lowered to 77 °K. The band was observed in all samples investigated; its origin is not yet understood. Because of the observed temperature dependence, it is tempting to associate this broad background with a "ferroelectric mode." Its existence is definitely incompatible with standard group-theoretical treatment of the ferroelectric phase crystal symmetry. The $A_1(z)$ lattice vibration, which is missing in the Raman spectrum, has been observed in the infrared[6] at 186 cm^{-1} with a 21-cm^{-1} room-temperature linewidth. This is considerably narrower than the 160-cm^{-1} linewidth observed in the $z(yy)x$ spectra. The fact that the long-wavelength $A_1(z)$ lattice mode was not observed indicates that the polarizability tensor components α_{xx}, α_{yy}, and α_{zz} associated with this mode are extremely small compared with the other fundamental A_1 phonons.

The spectrum which exhibited the largest number of extra depolarized lines was that taken in

TABLE I. 77 and 294 °K resonant frequencies and mode assignments for various orientations and polarizations of the incident and scattered photons in $NaNO_2$. The first six mode types are lattice modes, and the last three are internal molecular modes.

Observed Raman frequencies, ν in cm^{-1}				Mode symmetry and type
Orientation (°K)	$z(xx)y$	$z(yy)x$	$y(zz)x$	$A_1(z)$
ν at 77	Not obs.	Not obs.	Not obs.	Translational
ν at 294	Not obs.	Not obs.	Not obs.	vibration
Orientation (°K)	$z(yx)y$	$x(yx)y$	$x(yx)z$	A_2
ν at 77	127			Orientational
ν at 294	120	121	121	vibration
Orientation (°K)	$z(xz)y$	$z(xz)x$	$y(xz)x$	$B_1(x)$
ν at 77	161	164	157	Translational
ν at 294	153	159	152	vibration
ν at 77	207	205	176	$B_1(x)$
ν at 294	190	192	165	Orientational vibration
Orientation (°K)	$z(yz)x$	$z(yz)y$	$y(zy)x$	$B_2(y)$
ν at 77	157	180	180	Translational
ν at 294	142	169	168	vibration
ν at 77	242	243	231	$B_2(y)$
ν at 294	227	228	218	Orientational vibration
Orientation (°K)	$z(xx)y$	$z(yy)x$	$y(zz)x$	$A_1(z)$
ν at 77	832	832	828	Symmetric
ν at 294	828	828	832	bending vibration
ν at 77	1334	1337	1330	$A_1(z)$
ν at 294	1327	1330	1333	Symmetric stretch vibration
Orientation (°K)	$z(xz)y$	$z(xz)x$	$y(xz)x$	$B_1(x)$
ν at 77	1228	1296	1304	Asymmetric
ν at 294	1226	1296	1300	stretch vibration

the $y(zy)x$ orientation, where group theory predicts the existence of two phonons of type $B_2(y)$. The scattering intensity from this orientation is approximately one-tenth that of the $z(yz)x$ and the $z(yz)y$ orientation. Therefore, the gain was increased by a factor of 10 for the $y(zy)x$ spectrum. Inspection of this spectrum shown in Fig. 2 reveals the existence of five lines. Three of the extra lines in this particular spectrum are affixed with wave numbers. The lines at 180 and 231 cm^{-1} have been assigned to the $B_2(y)$ modes, while those at 127 and 165 cm^{-1} are attributed to the depolarized A_2 orientational vibration and the $B_1(x)$ translational vibration, respectively. The origin of the line at 276 cm^{-1} is not known. An attempt to track these lines from the $y(zy)x$ to the $y(zy)z$ configurations was met with little success because our instrumentation was such that we could not eliminate the strong A_2 mode which dominated the spectrum. With the exception of line broadening, the room-temperature spectrum obtained in the $y(zy)x$ orientation was similar to that shown at 77 °K.

As expected, the general effect on the phonons of lowering the crystal temperature to 77 °K is to raise their frequency and decrease their linewidth. None of the observed modes appear to become Raman inactive as the crystal makes the transition[5] to the low-temperature phase below 178 °K.

Frequency shifts as a function of the orientation of the phonon propagation vector with respect to the crystallographic axis have been observed in all five modes which are antisymmetric with respect to a twofold rotation about the polar C_2 axis (that is, all modes of type B). The results are tabulated in Table I. This result differs from that of Tramer, who observed orientational shifts in only three of the five asymmetric B modes. The greatest absolute shift was observed to occur in the $B_1(x)$ asymmetric stretching vibration of the NO_2^- molecular ion. The vibrational frequency varied from 1226 to 1360 cm^{-1}. Because of the large magnitude of this shift, this mode was selected for more detailed study at this time. As noted above, the other two $B_1(x)$ modes and the two $B_2(y)$ modes also exhibited orientational shifts, but of smaller amounts.

Frequency Shift of Internal $B_1(x)$ Modes as a Function of Phonon Wave-Vector Direction in the Crystal

Tramer[3] first noted frequency shifts with wave-vector orientation in sodium nitrite. He indicated that the shift depended upon the angle θ between the propagation direction and the phonon polarization direction and suggested an expression for the frequency as a function of θ, first derived by Poulet[9] for "piezoelectric noncubic" crystals. The approximate expression for relatively small frequency shift was given as

$$\nu = \nu_t + (\nu_l - \nu_t)\cos^2\theta,$$

where $\nu_t \equiv$ frequency for the transverse optical phonon, $\nu_l \equiv$ frequency for the longitudinal optical phonon, and $\theta \equiv$ angle between the phonon propagation

direction and the phonon polarization direction. The above expression is essentially the same as the approximate formulas for extraordinary phonons derived by Loudon[8] for *uniaxial* crystals, except for the values inserted for ν_t and ν_l. The values of these frequency parameters in Loudon's more complete treatment depended upon the dominance of either the long-range electrostatic forces or the short-range anisotropic forces. It should be emphasized here that the authors restricted their treatment to a simple dipolar complex in *uniaxial* crystals with only three infrared-active vibrations. The applicability of these frequency expressions to $NaNO_2$ is questionable, since there are eight infrared vibrational modes in this crystal. The above analysis applies only to crystals where only three infrared vibrational modes occur. In addition, $NaNO_2$ is *biaxial*. The theoretical expression for frequencies for biaxial crystals should, of course, be more complicated because there are three nonequivalent directions instead of just two as in the uniaxial system. Thus, in general, two angles are necessary to describe the wave-vector orientation and consequently the phonon frequency shift. However, the frequency of the asymmetric internal vibration

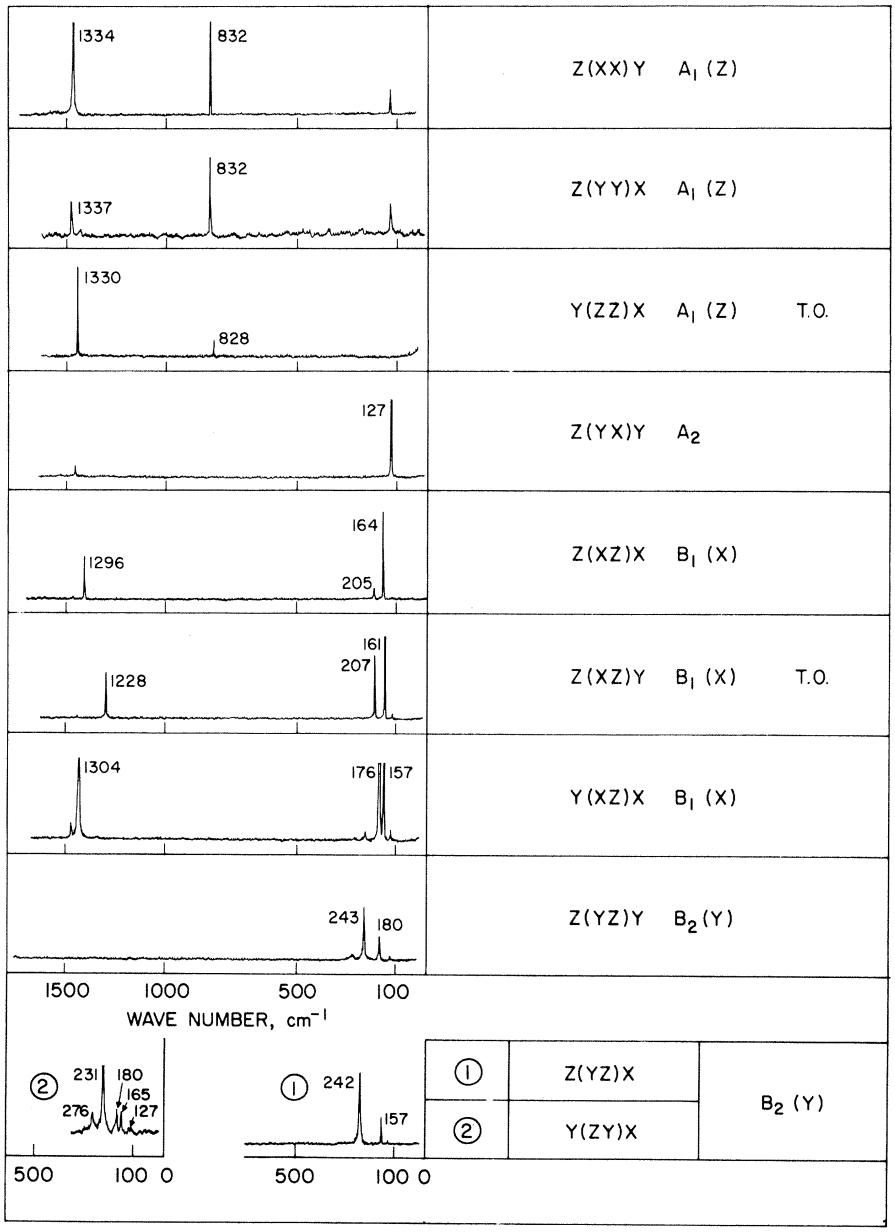

FIG. 2. Raman spectra of $NaNO_2$ at 77 °K for various orientations and polarizations of the incident and scattered light beams.

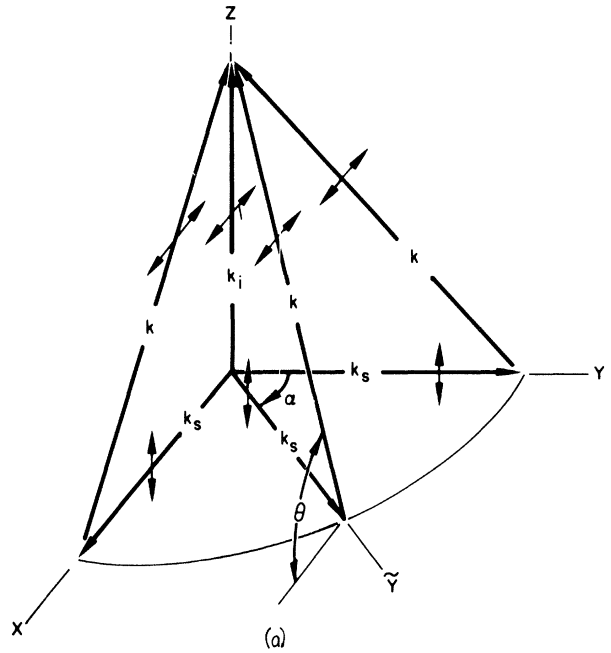

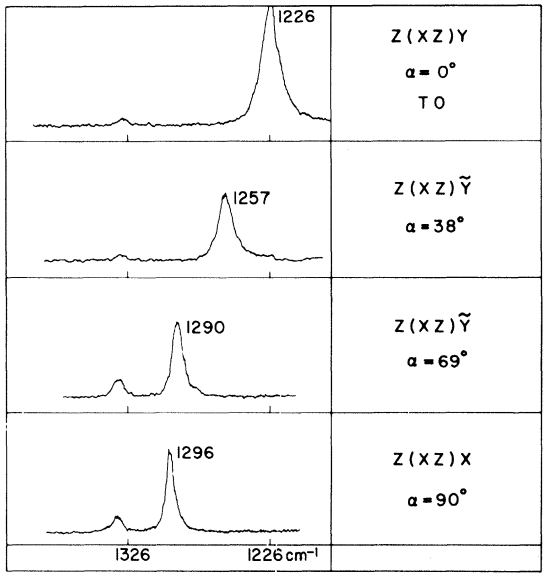

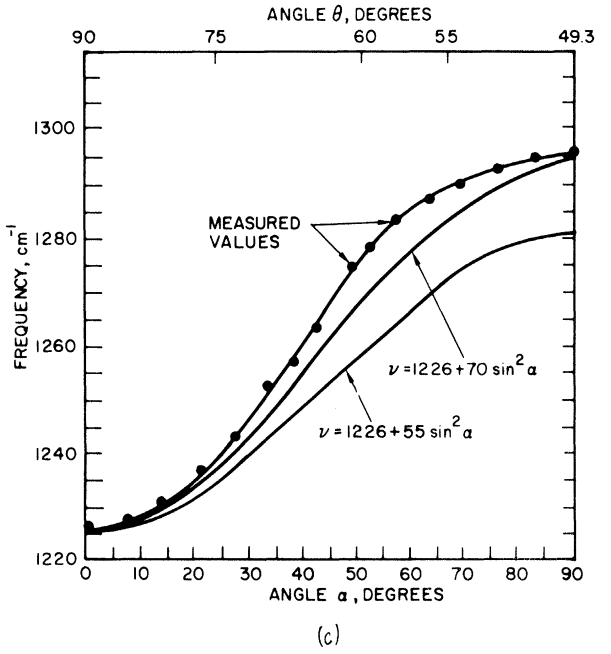

FIG. 3. (a) Polarization and orientation of the photon and phonon propagation wave vectors with respect to the crystal axes $\vec{k}_i$: incident photon; $\vec{k}_s$: scattered photon; $\vec{k}$: optical phonon. α is the angle between the y axis and $\vec{k}_s$. The $B_1(x)$ phonon is polarized along x. When the $\vec{k}_s$ direction is along y, a pure transverse wave is excited, whereas when the $\vec{k}_s$ direction is along x, a mixed transverse-longitudinal wave occurs. θ is the angle between the phonon propagation direction and the phonon polarization direction. (b) Spectra of the phonon frequency shifts with propagation direction change. The $B_1(x)$ mode, the asymmetric internal vibration of the NO_2^- molecule near 1250 cm^{-1}, exhibited a large frequency shift with changing phonon propagation direction. The mode is observed with the $z(xz)\tilde{y}$ scattering, where $\tilde{y}$ lies in the xy plane. The $B_1(x)$ mode frequency change as the propagation direction is rotated about the z axis by the angle α from the zy plane is shown for $\alpha = 0°$, 38°, 69°, and 90°. The weak line near 1330 cm^{-1} is a depolarized $A_1(z)$ component. (c) Frequency of the $B_1(x)$ mode as a function of the angle α and θ for the geometry of (a). The two simplified theoretical curves discussed in the text are shown.

$B_1(x)$ of the NO_2^- molecular ion appears to be approximately describable as a function of a single angle θ, the angle between the phonon wave vector and the phonon polarization direction. The fact that this mode is energetically isolated from the other eight normal modes, with the exception of the $A_1(z)$ internal vibration at 1330 cm^{-1}, may be related to this behavior.

It should not be inferred that the frequency shifts of all the types B normal modes can be approximately described by a simple function of the angle θ alone. This type of orientational dependence was definitely not observed in the other two $B_1(x)$ lattice vibrations. The observed orientational shifts of the two $B_2(y)$ normal modes also appear to be more involved. Detailed studies of the observed orientational shifts of the other asymmetric modes are in progress and will be reported in a later publication.

Frequency Shift for Phonon Vectors Inclined at 40.7° to z Axis

We have measured the frequencies of the internal $B_1(x)$ mode for phonon wave vectors inclined at an angle of 40.7° with the crystallographic z axis. The geometry is shown in Fig. 3(a). The incident photon wave vector denoted by $\vec{k}_i$ is directed along the z axis and polarized in the xy plane so that a large x component of polarization occurs. The scattered photon wave vector denoted by $\vec{k}_s$ lies in the xy plane, with its polarization direction taken parallel to the z axis. The phonon wave vector thus lies in the plane defined by $\vec{k}_i$ and $\vec{k}_s$ and is inclined at an angle of 40.7° to the z axis. As the angle α between $\vec{k}_s$ and the y axis is increased, the phonon wave vector rotates about the z axis from the zy plane to the zx plane.

The crystals used were cut into rectangular parallelepipeds with faces perpendicular to the crystallographic x, y, and z axes. Instead of rotating the directions of observation of the scattered light with the crystal kept stationary, the crystal was rotated about the z axis and the direction of observation was fixed. Refraction of the scattered wave at the obliquely positioned crystal face required a minor calculation to determine the correct angle α shown in Fig. 3(a).

The angle of 40.7° formed by the phonon wave vector $\vec{k}$ and the z axis was determined by the momentum conservation triangle formed by $\vec{k}_s$, $\vec{k}_i$, and $\vec{k}$. For this biaxial crystal the magnitudes of $\vec{k}_s$ and $\vec{k}_i$ are not equal. However, their ratio is approximately equal to the ratio of the refractive indices for their respective polarizations, that is, $|k_s|/|k_i| \simeq n_z/n_x = 0.860$. The phonon wave vector $\vec{k}$ then forms an angle of 40.7° with the z axis and an angle of 49.3° with the xy plane. Since we are interested only in photons polarized along the z and x directions, the shape and size of the triangle do not change as the crystal is rotated, as can be seen by considering the index ellipsoid[10] for biaxial crystals.

The spectra obtained for four different phonon wave-vector orientations are shown in Fig. 3(b). The uppermost spectrum shows the internal $B_1(x)$ line when the phonon wave vector lies in the zy plane. Because the phonon polarization direction is along x, the transverse optical frequency is observed, that is, $\nu_t = 1226$ cm^{-1}. The bottom spectrum of Fig. 3(b) shows the $B_1(x)$ line at 1296 cm^{-1} when the phonon wave vector lies in the zx plane. The middle two lines are for phonon wave vectors at intermediate positions. The lower three spectra give mixed L O and TO modes.

The results for phonon wave vectors inclined at 40.7° to the z axis for various other values of the angle α are shown in Fig. 3(c), where the frequency shifts versus the angle are plotted. The results obtained have also been compared with those calculated on the basis of Poulet's formula. The longitudinal-optical frequency ν_l for this mode is approximately 1360 cm^{-1} (see below). The angle θ between the phonon wave vector $\vec{k}$ and the phonon polarization direction [shown in Fig. 3(a)] can be easily expressed in terms of the angle α. The resulting formula is

$$\nu = \nu_t + (\nu_l - \nu_t)\, 0.420 \sin^2\alpha$$
$$= 1226 + 55 \sin^2\alpha \text{ cm}^{-1},$$

where the approximate ν_l value has been used. As can be seen in Fig. 3(c) the calculated values deviate from the measured values by as much as 35 cm^{-1}. If ν_l is arbitrarily set at $\nu_l = 1396$ cm^{-1}, the resulting expression $\nu = 1226 + 70 \sin^2\alpha$ fits the experimental points more closely in the θ range between 49.3° and 90°; however, deviations outside this range are much greater. Thses curves show that the θ dependency for this $B_1(x)$ line is nearly correct as given above, but that another parameter is necessary for closer fit to the experimental points.

Frequency of Approximately Longitudinal-Optical Phonon

In order to obtain an approximate value for the longitudinal-optical $B_1(x)$ internal phonon frequency, a crystal was cut in the orientation shown in Fig. 4(a). The cut faces are normal to the xy plane and inclined at 45° with respect to the x and y axis. The incident and scattered photon vectors were directed perpendicular to these faces. The phonon wave vector is thus nearly parallel to the x axis. Reversing the direction of one of the photon wave vectors will result in the phonon wave vector nearly aligned parallel to the crystallographic y axis.

Because the incident photon beam is polarized in the xy plane, it refracts away from the normal as it enters the birefringent crystal. The beam direction is, of course, along the direction of energy flow or the Poynting vector direction. However, the photon wave-vector direction is still perpendicular[10] to the crystal face, as indicated by $\vec{k}_i$ in Fig. 4(a).

Because momentum must be conserved, there is a deviation of the phonon direction from the x axis, or the $B_1(x)$ phonon polarization direction, owing to the change in the relative magnitudes of the $\vec{k}_i$ and $\vec{k}_s$. Figure 4(b) shows the calculated 4.7° angular deviation of the phonon wave vector $\vec{k}$ from the x-axis direction. Here again the ratio $|k_s|/|k_i|$ is 0.860, as mentioned previously. The spectrum is shown in Fig. 5.

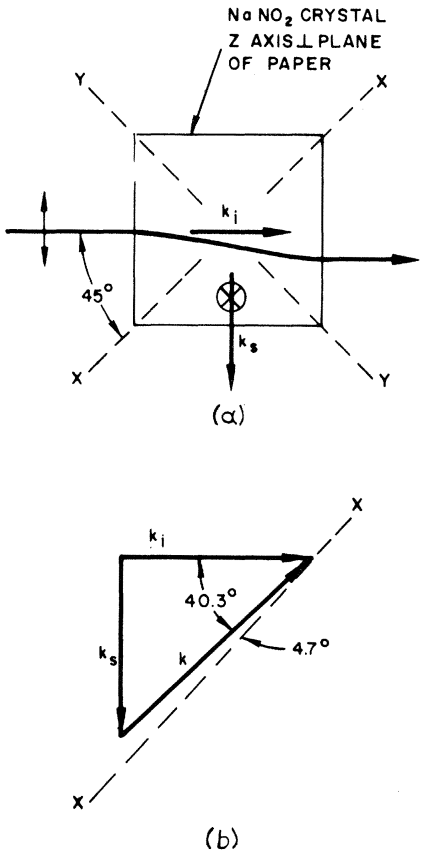

FIG. 4. (a) Orientation of the crystal for the measurement of the approximately LO frequency, and (b) $\vec{k}$ wave-vector triangle.

Frequencies for Phonon Vectors Inclined at an Angle of 49.3° to x Axis; Linewidth

Tramer's data indicated that there is no cylindrical symmetry of the phonon frequency about the x axis for those phonon wave vectors inclined at an angle of 45° to the x axis. He obtained a frequency of 1288 cm^{-1} for the 45° vector in the xz plane and 1310 cm^{-1} for the 45° vector in the xy plane. Our measurements gave values of 1296 and 1300 cm^{-1}, respectively, for these orientations, which is a more symmetrical result. However, the angle of 45° also must be corrected as discussed for the $\vec{k}$ wave-vector triangle described above. The phonon-vector inclination angle with the x axis is thus 49.3°. These two phonon vectors inclined equally to the x axis gave almost the same frequency values. The frequencies for intermediate vectors inclined at 49.3° with the x axis were not measured.

Finally, the linewidth and frequency for the four phonon wave-vector orientations are tabulated in column four of Fig. 6. The TO phonon with wave vector lying in the (zy) plane has a linewidth of 12 cm^{-1}, whereas the approximately LO phonon exhibits a linewidth of 2.9 cm^{-1}, a decrease by a factor of 4. The mixed TO + LO phonons exhibit intermediate linewidths.

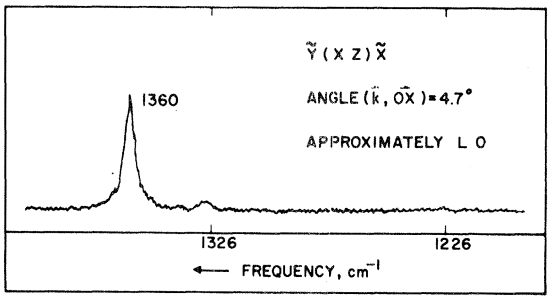

FIG. 5. Spectrum of the approximately LO $B_1(x)$ internal symmetric phonon. $\tilde{y}$ and $\tilde{x}$ denote that the incident and scattered photons are in the xy plane.

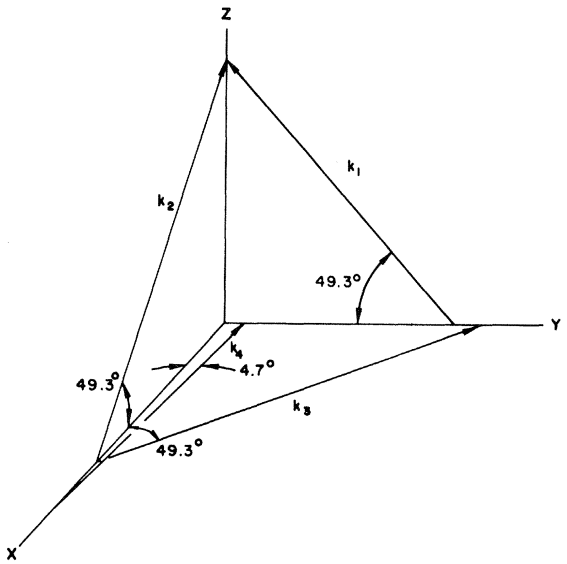

WAVE VECTOR $\vec{k}$	FREQUENCY ν	LINE WIDTH	TYPE OF WAVE
k_1	1226 cm^{-1}	12 cm^{-1}	TO
k_2	1296	4.3 cm^{-1}	TO + LO
k_3	1300	6.9 cm^{-1}	TO + LO
k_4	1360	2.9 cm^{-1}	APPROX. LO

FIG. 6. Diagram of the orientation of four particular phonon wave vectors in the x, y, z crystallographic coordinates. The frequencies, linewidths, and types of wave are listed.

SUMMARY AND CONCLUSIONS

The complete Raman spectra of $NaNO_2$ at 294 and 77°K have been presented here. There were no major differences in the spectra at the two temperatures, except for the expected sharpening of the lines at 77°K. The Raman spectrum was not affected by the phase transition at 178°K, as reported from thermal-expansion and low-frequency dielectric-constant measurements; the indicated phase transition does not appear to change the C_{2v} crystal symmetry at the lower temperature. The weak broad bands at low frequencies, which appear in the $A_1(z)$ spectra at 294°K, are not observed in the 77°K spectra. The low-frequency $A_1(z)$ mode at 186 cm^{-1} still has not been observed in the Raman spectra.

Frequency shifts with phonon propagation vector orientational changes were observed for all of the five asymmetric modes. The frequency change versus phonon-vector change of the asymmetric internal vibrational $B_1(x)$ mode of the nitrite molecule was studied in some detail; the frequency shift versus angle between the phonon propagation vector and the phonon polarization vector were measured. The linewidths of this mode for four phonon-vector orientations are given. Further experimental and theoretical study of this relatively simple biaxial crystal appears to offer an interesting way to probe the properties of lattice and internal vibrations in biaxial crystals. It should be determined why only the asymmetric vibrations show the large frequency shifts with change in the phonon-vector orientation.

ACKNOWLEDGMENTS

The authors are greatly indebted to R. J. Morrison and R. P. Lavery for construction of equipment and technical assistance, and to A. C. Pastor and R. C. Pastor for their crystal-growing effort.

---

[1]E. V. Chisler and M. S. Shur, Phys. Status Solidi 17, 163 (1966).
[2]E. V. Chisler and M. S. Shur, Phys. Status Solidi 17, 173 (1966).
[3]A. Tramer, Compt. Rend. 248, 3546 (1959). Note that the author's x, y, z corresponds to our x, z, y, respectively.
[4]Y. Yamada, I. Shibuya, and S. Hoshino, J. Phys. Soc. Japan 18, 1594 (1963).
[5]K. Gesi, J. Phys. Soc. Japan 26, 953 (1969).
[6]M. K. Barnoski and J. M. Ballantyne, Phys. Rev. 174, 946 (1968).
[7]J. D. Axe, Phys. Rev. 167, 573 (1968).
[8]R. Loudon, Advan. Phys. 13, 423 (1964).
[9]H. Poulet, Ann. Phys. (N. Y.) 12, 908 (1955).
[10]M. Born and E. Wolf, *Principles of Optics* (Pergamon, New York, 1959).